HHS Public Access

Author manuscript

Alzheimers Dement. Author manuscript; available in PMC 2019 June 01.

Published in final edited form as:

Alzheimers Dement. 2018 June ; 14(6): 764–774. doi:10.1016/j.jalz.2017.12.007.

Free water determines diffusion alterations and clinical status in cerebral small vessel disease

Marco Duering[a], **Sofia Finsterwalder**[a], **Ebru Baykara**[a], **Anil Man Tuladhar**[b], **Benno Gesierich**[a], **Marek J. Konieczny**[a], **Rainer Malik**[a], **Nicolai Franzmeier**[a], **Michael Ewers**[a], **Eric Jouvent**[c,d], **Geert Jan Biessels**[e], **Reinhold Schmidt**[f], **Frank-Erik de Leeuw**[b], **Ofer Pasternak**[g,*], and **Martin Dichgans**[a,h,i,*]

[a]Institute for Stroke and Dementia Research, Klinikum der Universität München, Ludwig-Maximilians-University LMU, Munich, Germany [b]Radboud University Medical Center, Donders Institute for Brain, Cognition and Behaviour, Department of Neurology, Nijmegen, The Netherlands [c]Univ Paris Diderot, DHU NeuroVasc Sorbonne Paris Cité, UMR-S 1161 INSERM, Paris, France [d]Assistance publique - hôpitaux de Paris (AP-HP), Lariboisière Hospital, Department of Neurology, Paris, France [e]Department of Neurology, Brain Center Rudolf Magnus, University Medical Center Utrecht, Utrecht, The Netherlands [f]Department of Neurology, Medical University of Graz, Graz, Austria [g]Departments of Psychiatry and Radiology, Brigham and Women's Hospital, Harvard Medical School, Boston, MA, USA [h]Munich Cluster for Systems Neurology (SyNergy), Munich, Germany [i]German Center for Neurodegenerative Diseases (DZNE), Munich, Germany

Abstract

Introduction—Diffusion tensor imaging detects early tissue alterations in Alzheimer's disease and cerebral small vessel disease (SVD). However, the origin of diffusion alterations in SVD is largely unknown.

Methods—To gain further insight, we applied free water (FW) imaging to patients with genetically defined SVD (CADASIL, n=57), sporadic SVD (n=444), and healthy controls (n=28). We modelled freely diffusing water in the extracellular space (FW) and measures reflecting fiber structure (tissue compartment). We tested associations between these measures and clinical status (processing speed and disability).

Results—Diffusion alterations in SVD were mostly driven by increased FW and less by tissue compartment alterations. Among imaging markers, FW showed the strongest association with

Correspondence to: Marco Duering, MD. Institute for Stroke and Dementia Research, Feodor-Lynen-Str. 17, 81377 Muenchen, Germany, Phone: +49 89 4400 46166, marco.duering@med.uni-muenchen.de.

*contributed equally as senior authors

Conflicts of interest

None

clinical status (R^2 up to 34%, P<.0001). Findings were consistent across patients with CADASIL and sporadic SVD.

Conclusions—Diffusion alterations and clinical status in SVD are largely determined by extracellular fluid increase rather than alterations of white matter fiber organization.

Keywords

small vessel disease; vascular cognitive impairment; structural imaging; diffusion tensor imaging; free water; processing speed; disability; white matter hyperintensities; lacunes; brain atrophy

1. INTRODUCTION

Cerebral small vessel disease (SVD) is the major cause of vascular cognitive impairment and an important contributor to cognitive decline in patients with Alzheimer's disease (AD) [1,2]. SVD typically manifests with widespread brain changes detectable by MRI [3]. Diffusion tensor imaging (DTI) has emerged as a key method for studying SVD [4]. By quantifying diffusion properties of water in tissue, DTI is highly sensitive in detecting early and subtle tissue alterations. The typical pattern in SVD is an increase in the extent of water diffusion (increased mean diffusivity, MD) and reduced directionality (decreased fractional anisotropy, FA). Moreover, DTI alterations are strongly associated with clinical deficits, both in cross-sectional [5,6] and in longitudinal studies [7]. In fact, DTI-based markers typically outperform other MRI measures with respect to clinico-radiological correlations [8].

Despite the wide use of DTI, little is known about the structural underpinnings of diffusion alterations in SVD, in part since DTI measures are not specific to a single pathology [9,10]. The prevailing interpretation is that the increased MD and reduced FA result from microstructural tissue damage, such as axonal degeneration and subsequent loss of white matter fiber organization [11]. However, recent data from experimental models and neuroimaging studies offer alternative explanations for altered water diffusion in SVD, such as edema caused by blood brain barrier damage [12,13] or vacuolization within myelin sheets [14]. The ability of the conventional DTI model to distinguish between these options is limited [15].

Recent advances in diffusion MRI modeling enable more detailed insight into DTI alterations. Of specific interest for SVD is the free water (FW) diffusion MRI model [16]. This technique enhances DTI by explicitly modeling a FW compartment, in addition to a tissue compartment (Fig. 1). The FW compartment represents water molecules that are not restricted or directed. It is modeled by a tensor that is isotropic and has a fixed diffusion coefficient of water at 37°C. The tissue compartment represents all remaining water molecules, i.e. water molecules within or in close proximity to cellular structures. This includes intracellular water as well as extracellular water affected by physical barriers, such as axon membranes and myelin. Hence, the tissue compartment reflects white matte fiber organization. While FW imaging was initially developed to correct the diffusion signal for cerebrospinal fluid contamination [17], the approach has recently been applied to study brain tumors [16], psychiatric disorders [18,19], and neurodegenerative diseases [18,20,21]. These studies indicate that FW imaging increases the sensitivity of DTI to identify clinically

relevant microstructural alterations [19,22]. Interestingly, in AD patients, alterations in the tissue compartment were found already at early disease stages and were associated with conversion to dementia [22].

In this study, we used FW imaging to obtain deeper insight into the underpinnings of diffusion alterations in SVD. We first explored the contribution of FW and the tissue compartment measures to diffusion alterations in SVD. We then analyzed the association between clinical status and both FW and tissue compartment measures. To minimize confounding from age-related pathologies, we evaluated young patients with the genetically defined SVD CADASIL (Cerebral Autosomal Dominant Arteriopathy with Subcortical Infarcts and Leukoencephalopathy), which is caused by mutations in *NOTCH3*. We further studied a large sample of sporadic SVD patients to validate our findings obtained in CADASIL and to address their generalizability towards sporadic SVD.

2. SUBJECTS AND METHODS

2.1. Subjects

CADASIL patients (n=57) and healthy control subjects (n=28) were recruited through an ongoing, prospective, single-center study in Munich [8]. CADASIL was confirmed by molecular genetic testing (identification of a cysteine-altering mutation in the *NOTCH3* gene by Sanger sequencing) or by ultrastructural analysis of a skin biopsy (detection of pathognomonic granular osmiophilic material on the surface of vascular smooth muscle cells). Control subjects met the following criteria: i) No history for neurological or psychiatric disease, ii) no cognitive complaints and no cognitive deficits on neuropsychological testing, iii) absence of confluent white matter hyperintensities (WMH) on MRI (Fazekas scale score ≤ 1).

Patients with sporadic SVD (n=444) were included from the RUN DMC (Radboud University Nijmegen Diffusion tensor and Magnetic resonance imaging Cohort) study. This prospective, single-center study recruited non-demented elderly (age 50–85) with SVD, defined as the presence of lacunes and/or WMH on neuroimaging. Patients were recruited in a hospital-based setting. The main reasons for referral to the hospital were acute (e.g. transient ischemic attack, stroke presenting with lacunar syndrome) or subacute symptoms of SVD (e.g. cognitive and/or gait disturbances). Main exclusion criteria were baseline parkinsonism, dementia, life expectancy of less than 6 months and non-SVD-related white matter lesions (e.g. multiple sclerosis). More details can be found in the previously published study protocol [23]. Both studies were approved by the ethics committees of the respective institutions. Written informed consent was obtained from all subjects.

2.2. Cognitive and clinical assessment

Neuropsychological testing was performed on the same day or the day before MRI scanning (CADASIL patients) or within three weeks before MRI (sporadic SVD, RUN DMC study), respectively. Processing speed was quantified using compound scores obtained from the cognitive test batteries of the two samples. In CADASIL patients and control subjects, the compound score was based on the two trail making tests (matrix A and B). In sporadic SVD

patients, the compound score was based on the 1-letter subtask of the Paper-Pencil Memory Scanning Test and the Letter-Digit Substitution Task. Raw scores were transformed to age and education-corrected z-scores based on normative data obtained from literature [24–26], and the compound score was calculated by averaging the z-scores. Five sporadic SVD patients from the RUN DMC study had missing neuropsychological data. Data on disability as assessed by the modified Rankin scale was available for CADASIL patients.

Arterial hypertension was defined as systolic blood pressure ≥140 mmHg and/or diastolic blood pressure ≥90 mmHg and/or use of an antihypertensive drug. Diabetes and hypercholesterolemia were defined as use of an antidiabetic or lipid-lowering drug for high cholesterol, respectively.

2.3. MRI and conventional SVD imaging markers

The MRI protocols in both studies included 3D-T1, T2, fluid-attenuated inversion recovery, gradient echo (T2*), and diffusion MRI sequences (30 directions; Munich: TR/TE 12700ms/81ms, b-value 1000 s/mm^2, 2 mm isotropic resolution; RUN DMC: 10100ms/93ms, 900 s/mm^2, 2.5 mm isotropic). Complete details on sequence parameters are provided in Supplementary Table 1.

We used consensus criteria [3] to assess the following conventional SVD imaging makers: WMH volume, lacune volume, number of cerebral microbleeds, and brain volume using published segmentation pipelines [5,8,27]. All volumes were normalized for head size by the intracranial volume.

2.4. Diffusion Measures

After visual quality control, raw diffusion images were first corrected for eddy current induced distortions and head motion as previously described [8,28]. Diffusion tensors were estimated from the preprocessed diffusion MRI data using linear least squares implemented in Matlab. The conventional DTI measures of MD and FA were calculated from the tensors for each voxel using fslmaths, part of FSL (Functional Magnetic Resonance Imaging of the Brain software library), version v5.0.9 [29]. FW maps as well as tissue compartment diffusion tensors were estimated using a non-linear regularized minimization process implemented in Matlab [16]. Briefly, in each voxel the signal was fitted to a two-compartment model (Fig. 1), including a FW compartment (isotropic tensor with fixed diffusion constant of water at 37 °C) and a tissue compartment (FW-corrected tensor). The estimated parameters were the fractional volume of the FW compartment (i.e. the FW measure) and the tensor of the tissue compartment. The FW measure expresses the relative contribution of FW in each voxel, ranging from 0 to 1. The tensor of the tissue compartment reflects the tissue microstructure after removing the signal contributed by FW. From this tensor, the tissue compartment measures of MDt and FAt were calculated using fslmaths. Global alterations of diffusion measures were assessed on the white matter skeleton, which was obtained by the Tract-Based Spatial Statistics procedure [30], part of FSL. The skeleton (generated with a FA threshold of ≥0.2) and a custom-made mask [8] were used to exclude areas that are prone to cerebrospinal fluid contamination. By restricting the analysis to white matter tracts with FA values above 0.2, lacunes (fluid-filled cavities with signal identical to

cerebrospinal fluid) were excluded from the analysis. The mean of all voxels in the masked skeleton was used as a global measure for further analysis.

Cerebral microbleeds can be abundant in CADASIL patients [31], and might influence the diffusion signal as assessed by echo planar imaging. Importantly, in our study, there was no indication that microbleeds interfered with the analysis of diffusion measures within main fiber tracts, as most of them were outside tracts and had no measureable effect on the diffusion signal.

2.5. Statistical analysis

All statistical analyses were performed in R (version 3.2.4) [32]. Comparisons between groups were performed with one-way analysis of variance (ANOVA) and Tukey's post hoc test (normally distributed data), Kruskal-Wallis test and Nemenyi's post-hoc test (skewed or ordinal data), or fisher exact test (binary data), as appropriate. Post-hoc-tests were corrected for multiple comparisons.

To facilitate the interpretation of group differences (CADASIL vs. controls) across the different diffusion measures, all values were standardized using the mean and standard deviation of the control group. For sporadic SVD, we split the sample into quartiles according to the WMH volume and used mean and standard deviation of patients with low SVD lesion burden (i.e. the first quartile of WMH volume) for standardization.

To assess how alterations in FW and the tissue compartment measures (FAt, MDt) may explain alterations in the global, conventional DTI measures (FA, MD), we used partial regression with the conventional DTI measure as the dependent variable. The ability of diffusion measures to discriminate between CADASIL and controls was assessed using receiver operating characteristic analysis as implemented in the R package 'ROCR' (version 1.0–7) [33]. Area under the curve (AUC) values, including 95% confidence intervals, are given after 5-fold cross validation.

Associations between imaging measures and processing speed were first assessed by simple linear regression analysis. Processing speed scores were power transformed to achieve normal distribution. In the RUN DMC sample, one subject was excluded for regression analysis after a Bonferroni-adjusted regression outlier test (as implemented in the R package 'car') [34] in order to ensure that regression results were not driven by this single outlier. In addition, we aimed to determine the relationship of all imaging markers, as well as age and sex, with clinical status. Because of high intercorrelations among these variables (multicollinearity), we did not perform multiple linear regression to avoid the associated risks of overfitting, overadjustment and ultimately biased estimation [35,36]. Instead, we used random forest regression, which assesses the explanatory power of variables while accounting for all other variables. This recursive partitioning technique can deal with large numbers of independent variables, even in the presence of complex interactions and multicollinearity, when applying conditional inference trees [37]. Using the R package 'party' (version 1.0–25) [38] we calculated 1501 conditional inference trees with unbiased variable selection using standard parameters (5 randomly preselected variables for each split, unbiased resampling scheme). From these trees we next calculated a conditional permutation

importance (following the permutation principle of the 'mean decrease in accuracy' importance measure) [39] for each variable together with a 95% confidence interval from 400 repetitions.

Associations between imaging measures and disability, as assessed by the modified Rankin scale, were analyzed using ordinal logistic regression (R package 'ordinal') and random forest regression.

3. RESULTS

Demographic characteristics of the study samples are presented in table 1. CADASIL patients were younger than control subjects and had higher WMH volumes. Lacunes (n=40 patients [70%]) and microbleeds (n=25 [44%]) were common in CADASIL patients but absent in control subjects.

3.1. Free water is the main contributor to DTI alterations in genetically defined SVD

Figure 2A shows an example of the conventional FA maps, FW maps, and tissue compartment FAt maps in a representative CADASIL patient and a representative control subject. The CADASIL patient exhibited regions of substantially lower FA compared with the control subject. There was a large increase in FW in these regions whereas differences in FAt were much less pronounced.

When comparing the diffusion measures in the entire group of CADASIL patients with controls (Fig. 2B), we found a marked reduction in global white matter FA and increase in MD in line with earlier DTI studies. The difference was markedly smaller for tissue compartment measures, and FW showed the most prominent increase in CADASIL patients. A similar pattern was found when analyzing normal appearing white matter and WMH separately (Supplementary Results 1, Supplementary Fig. 1A). Overall, alterations in normal appearing white matter were less pronounced, with tissue compartment FAt showing almost no difference compared with controls. FW showed the largest increase both in normal appearing white matter and in white matter hyperintensities. Results of a voxelwise analysis in a representative CADASIL patient are presented in Supplementary Results 2 (Supplementary Fig. 2).

To further understand how changes in FW and the tissue compartment may explain changes in conventional FA and MD we used partial regression (Fig. 2C). Variability of conventional FA was determined predominantly by FW and to a lesser extent by the tissue compartment FAt. Conventional MD was almost entirely determined by alterations in FW with only minimal contribution from the tissue compartment MDt.

As expected, conventional FA and MD provided excellent classification of CADASIL patients from controls (Fig. 2D). The tissue compartment measures FAt and MDt were also good classifiers, but AUCs were noticeably lower than those of FA and MD. The AUC of FW was the highest of all measures, suggesting that the high classifier performance of conventional FA and MD mostly originated from FW signal included within these conventional measures.

3.2. Validation in sporadic SVD

To address the generalizability of these findings towards sporadic disease, we next analyzed SVD patients recruited through the RUN DMC study. The study sample was split into quartiles according to WMH volume. As expected, the global FA decreased while the global MD increased with increasing disease burden (Fig. 3A). Similar to the CADASIL sample, the group differences were less pronounced for the tissue compartment measures, and FW showed the largest difference between groups. As in CADASIL patients, partial regression in the entire sporadic SVD sample (Fig. 3B) showed that alterations of conventional FA in major white matter tracts were driven both by FW and FAt, while MD was almost entirely determined by FW with only minor contribution from MDt. Again, a similar pattern was found when analyzing normal appearing white matter and WMH separately (Supplementary Results 1, Supplementary Fig. 1B).

3.3. Free water is strongly associated with clinical deficits

Next, we assessed the relationship of FW, tissue compartment measures (FAt, MDt), and other quantitative MRI markers (WMH volume, lacune volume, brain volume, cerebral microbleed count) with clinical deficits (cognitive function and disability). For cognitive function, we focused on processing speed as the most prominently affected cognitive domain in patients with SVD [40,41].

Table 2 depicts the results from simple linear regression analyses with processing speed as the dependent variable. FW was the diffusion measure having the strongest association with processing speed both in CADASIL patients and in patients with sporadic SVD. A subgroup analysis for sporadic SVD patients with high disease burden (4^{th} quartile) showed increased effect sizes and explained variance compared with the entire sample. Regression plots for the speed score and FW for CADASIL patients and for sporadic SVD patients (4^{th} quartile) are presented in Fig. 4A.

Correlation matrices revealed a high intercorrelation among imaging markers and between imaging markers and age (Fig. 4B). Therefore, to assess the contribution of each imaging marker to processing speed performance while accounting for intercorrelations (multicollinearity), we applied random forest regression and calculated the conditional variable importance. The FW measure had the highest variable importance both in CADASIL patients and in sporadic SVD patients with high disease burden (4^{th} quartile) (Fig. 4C). Other variables showing a reasonably consistent contribution to processing speed in both samples were the FAt and lacune volume, although their variable importance was considerably lower than for FW. Because of smaller effect sizes, results in the entire sporadic SVD sample were unstable with largely overlapping confidence intervals (data not shown).

Similar results were found for disability as measured by the modified Rankin Scale score in the CADASIL sample (Supplementary Table 2). Simple ordinal logistic regression showed that the most significant association was between FW and the modified Rankin Scale score ($P \approx 4.43 \times 10^{-6}$). Also, FW had the highest conditional variable importance in random forest regression (Supplementary Fig. 3).

4. DISCUSSION

This study applied FW imaging to explore the underpinnings of diffusion MRI alterations in cerebral SVD. The main findings can be summarized as follows: i) DTI alterations, i.e. reduction in FA and increase in MD, were mostly driven by increased FW; ii) Compared with FW, alterations in the tissue compartment were relatively mild; iii) Among all imaging markers, FW showed the strongest association with clinical deficits. Importantly, all results were consistent across patients with genetic and sporadic SVD. Taken together, these *in vivo* findings provide new insights into cerebral SVD and define FW as a clinically relevant target for future research.

Our results represent a major step forward in the interpretation of SVD-related diffusion imaging changes on the tissue level. The FW signal suggests a substantial increase of water within white matter with properties similar to cerebrospinal fluid, i.e. unrestricted and undirected (isotropic) water diffusion at 37°C. The increase in FW content was found both in white matter hyperintensities and in white matter appearing normal on T2 imaging, suggesting that FW elevation might be an early event. The relatively mild alterations in the tissue compartment, reflecting fiber structure, suggest that the organization of white matter fiber tracts was relatively preserved in our patients. These findings contrast with traditional explanations for diffusion imaging alterations in SVD. Furthermore, these results suggest that DTI alterations in SVD have different underpinnings than in AD, where changes were predominantly found in the tissue compartment [22].

The precise factors leading to the observed increase of extracellular water and hence increased FW signal in SVD remain to be determined. Possible explanations include vasogenic edema and intramyelinic vacuolization. Recent studies both in experimental models and in humans provide evidence for a disruption of the blood-brain barrier and subsequent vasogenic edema in SVD. CADASIL (*Notch3*-R169C) transgenic mice develop a loss of pericytes, reduced astrocytic endfeet coverage, and blood-brain barrier breakdown as demonstrated by leakage of plasma proteins into brain tissue [12]. Also, mice deficient for *Foxf2*, a gene recently linked to SVD, exhibit breakdown of the blood-brain barrier together with deficits in pericyte maturation [42]. In humans, data from neuropathological studies are conflicting regarding the extravasation of plasma proteins in SVD [43,44], with one study finding plasma extravasation to be common in aged brains but having no association with neuropathological markers of SVD [45]. Meanwhile, there is accumulating *in vivo* evidence for a disruption of the blood-brain barrier in SVD patients from dynamic contrast enhanced imaging [13]. These studies have demonstrated increased blood-brain barrier leakage both in patients with SVD related stroke [46–48] and in patients with SVD related vascular cognitive impairment [48,49].

Another possible explanation for the observed increase in FW is intramyelinic vacuolization, which was likewise described in CADASIL transgenic mice and interpreted as intramyelinic edema resulting from compromised ion and water homeostasis [14]. In larger vacuoles, water will be able to move without restriction and therefore increase the FW signal. However, the precise mechanisms underlying vacuolization remain unknown and it is possible that fluid-filled vacuoles within myelin occur as a result of demyelination. While

neuropathology studies in humans have provided clear evidence for demyelination in SVD [11], intramyelinic vacuolization has so far not specifically been studied. Of note, segmental vacuolization was among the earliest abnormalities in CADASIL transgenic mice [14]. Hence, this may be difficult to assess in post-mortem material of late-stage disease. While there is strong evidence for a role of vasogenic edema and vacuolization in SVD, we cannot exclude the possibility that additional factors, such as alterations in blood volume and flow, also contribute to increasing the FW measure.

The second major finding of our study is that structural damage to white matter fiber tracts seemed much less pronounced than suggested by conventional FA. With conventional DTI, all water is combined in the analysis. Thus, any increase in FW, e.g. from edema, results in an apparent loss of directionality of water diffusion [16]. Analyzing the tissue compartment, we found only small alterations in FAt. Interestingly, FAt values were largely unaltered in white matter appearing normal on T2 imaging, while conventional FA values were decreased. This suggests that the structures underlying directed water diffusion, i.e. membranes of axons and myelin sheets, are more preserved than previously thought, especially in normal appearing white matter. Human neuropathology studies draw a heterogeneous picture regarding axonal degeneration in SVD [11]. However, only a few studies have applied stereological methods, and a small study on WMH in elderly individuals found no difference in axon density within and outside WMH, thus concluding that axons are mostly preserved within WMH [50].

Nevertheless, the FW signal in SVD showed strong associations with clinical deficits, in particular cognitive impairment. In both study samples, random forest regressions identified FW as the most important factor among all variables including age, sex, and other imaging markers. Admittedly, it is difficult to conceptualize how an interstitial fluid increase alone could cause pronounced clinical deficits. Thus, one might speculate that increases in FW in part reflect demyelination without prominent axonal degeneration.

Limitations of our study include the cross-sectional design and the lack of data correlating DTI changes with histopathology. However, quantifying water distribution in post mortem tissue is extremely challenging, highly influenced by post-mortem interval, and almost impossible after fixation [51]. Also, we are not aware of any autopsy samples with available ante-mortem DTI acquired within a reasonable time frame. Another limitation is that control subjects were older than CADASIL patients. If anything, this may have resulted in an underestimation of the differences between CADASIL patients and controls (Supplementary Fig. 4). Differences in MRI field strengths, sequence parameters and cognitive assessment between the two patient samples might also be seen as a limitation. However, these differences can also be considered a strength in terms of independent validation and generalizability. Another strength is the use of random forest regression, accounting for inter-correlations and multicollinearity, thus enabling robust quantification of the contribution of each marker. A major asset, finally, is the inclusion of young patients with genetically defined SVD. This allowed us to largely exclude a confounding effect from age-related pathologies.

While FW imaging provides additional insights into the origin of DTI alterations, the conventional DTI measures still serve as good biomarkers. Alterations in the conventional MD are almost entirely driven by FW and are therefore a good proxy for the FW measure. A potential advantage of conventional MD over FW is the availability of established post-processing techniques providing high robustness and inter-scanner reliability [8].

In conclusion, our findings identify increased extracellular FW as the main source of diffusion alterations in SVD and suggest that the degeneration of white matter tracts may be less pronounced than previously assumed. These observations along with the strong association with clinical status define FW as an important target for future research.

Supplementary Material

Refer to Web version on PubMed Central for supplementary material.

Acknowledgments

This study was funded by a D-A-CH grant (German Research Foundation DFG DU1626/1-1, Austrian Science Fund FWF I2889-B31), the Alzheimer Forschung Initiative e.V. (#16018CB), the Else Kröner-Fresenius-Stiftung (2014_A200), the Vascular Dementia Research Foundation, European Union's Horizon 2020 research and innovation programme under grant agreement No 666881, SVDs@target, the Netherlands Organisation for Scientific Research (016.126.351), and the National Institutes of Health (MH108574, EB015902). Dr. Tuladhar is a junior staff member of the Dutch Heart Foundation (2016T044). Dr. de Leeuw is supported by a clinical established investigator grant of the Dutch Heart Foundation (2014 T060) and by a VIDI innovational grant from The Netherlands Organisation for Health Research and Development (ZonMw grant 016•126•351).

ABBREVIATIONS

DTI	diffusion tensor imaging
FA	fractional anisotropy
FW	free water
MD	mean diffusivity
SVD	small vessel disease
WMH	white matter hyperintensity

References

1. Pantoni L. Cerebral small vessel disease: from pathogenesis and clinical characteristics to therapeutic challenges. Lancet Neurol. 2010; 9:689–701. [PubMed: 20610345]
2. Dichgans M, Leys D. Vascular Cognitive Impairment. Circ Res. 2017; 120:573–91. [PubMed: 28154105]
3. Wardlaw JM, Smith EE, Biessels GJ, Cordonnier C, Fazekas F, Frayne R, et al. Neuroimaging standards for research into small vessel disease and its contribution to ageing and neurodegeneration. Lancet Neurol. 2013; 12:822–38. [PubMed: 23867200]
4. Pasi M, van Uden IW, Tuladhar AM, de Leeuw FE, Pantoni L. White Matter Microstructural Damage on Diffusion Tensor Imaging in Cerebral Small Vessel Disease: Clinical Consequences. Stroke. 2016; 47:1679–84. [PubMed: 27103015]

5. Tuladhar AM, van Norden AG, de Laat KF, Zwiers MP, van Dijk EJ, Norris DG, et al. White matter integrity in small vessel disease is related to cognition. NeuroImage Clinical. 2015; 7:518–24. [PubMed: 25737960]
6. de Laat KF, Tuladhar AM, van Norden AG, Norris DG, Zwiers MP, de Leeuw FE. Loss of white matter integrity is associated with gait disorders in cerebral small vessel disease. Brain. 2011; 134:73–83. [PubMed: 21156660]
7. Jokinen H, Schmidt R, Ropele S, Fazekas F, Gouw AA, Barkhof F, et al. Diffusion changes predict cognitive and functional outcome: the LADIS study. Ann Neurol. 2013; 73:576–83. [PubMed: 23423951]
8. Baykara E, Gesierich B, Adam R, Tuladhar AM, Biesbroek JM, Koek HL, et al. A Novel Imaging Marker for Small Vessel Disease Based on Skeletonization of White Matter Tracts and Diffusion Histograms. Ann Neurol. 2016; 80:581–92. [PubMed: 27518166]
9. O'Donnell LJ, Pasternak O. Does diffusion MRI tell us anything about the white matter? An overview of methods and pitfalls. Schizophr Res. 2015; 161:133–41. [PubMed: 25278106]
10. Jones DK, Cercignani M. Twenty-five pitfalls in the analysis of diffusion MRI data. NMR Biomed. 2010; 23:803–20. [PubMed: 20886566]
11. Gouw AA, Seewann A, van der Flier WM, Barkhof F, Rozemuller AM, Scheltens P, et al. Heterogeneity of small vessel disease: a systematic review of MRI and histopathology correlations. Journal of neurology, neurosurgery, and psychiatry. 2011; 82:126–35.
12. Ghosh M, Balbi M, Hellal F, Dichgans M, Lindauer U, Plesnila N. Pericytes are involved in the pathogenesis of cerebral autosomal dominant arteriopathy with subcortical infarcts and leukoencephalopathy. Ann Neurol. 2015; 78:887–900. [PubMed: 26312599]
13. Wardlaw JM, Smith C, Dichgans M. Mechanisms of sporadic cerebral small vessel disease: insights from neuroimaging. Lancet Neurol. 2013; 12:483–97. [PubMed: 23602162]
14. Cognat E, Cleophax S, Domenga-Denier V, Joutel A. Early white matter changes in CADASIL: evidence of segmental intramyelinic oedema in a pre-clinical mouse model. Acta Neuropathol Commun. 2014; 2:49. [PubMed: 24886907]
15. Talbott JF, Nout-Lomas YS, Wendland MF, Mukherjee P, Huie JR, Hess CP, et al. Diffusion-Weighted Magnetic Resonance Imaging Characterization of White Matter Injury Produced by Axon-Sparing Demyelination and Severe Contusion Spinal Cord Injury in Rats. J Neurotrauma. 2016; 33:929–42. [PubMed: 26483094]
16. Pasternak O, Sochen N, Gur Y, Intrator N, Assaf Y. Free water elimination and mapping from diffusion MRI. Magnetic resonance in medicine: official journal of the Society of Magnetic Resonance in Medicine/Society of Magnetic Resonance in Medicine. 2009; 62:717–30.
17. Metzler-Baddeley C, O'Sullivan MJ, Bells S, Pasternak O, Jones DK. How and how not to correct for CSF-contamination in diffusion MRI. Neuroimage. 2012; 59:1394–403. [PubMed: 21924365]
18. Pasternak O, Westin CF, Bouix S, Seidman LJ, Goldstein JM, Woo TU, et al. Excessive extracellular volume reveals a neurodegenerative pattern in schizophrenia onset. J Neurosci. 2012; 32:17365–72. [PubMed: 23197727]
19. Bergamino M, Pasternak O, Farmer M, Shenton ME, Hamilton JP. Applying a free-water correction to diffusion imaging data uncovers stress-related neural pathology in depression. NeuroImage Clinical. 2016; 10:336–42. [PubMed: 27006903]
20. Planetta PJ, Ofori E, Pasternak O, Burciu RG, Shukla P, DeSimone JC, et al. Free-water imaging in Parkinson's disease and atypical parkinsonism. Brain. 2016; 139:495–508. [PubMed: 26705348]
21. Ofori E, Pasternak O, Planetta PJ, Li H, Burciu RG, Snyder AF, et al. Longitudinal changes in free-water within the substantia nigra of Parkinson's disease. Brain. 2015; 138:2322–31. [PubMed: 25981960]
22. Maier-Hein KH, Westin CF, Shenton ME, Weiner MW, Raj A, Thomann P, et al. Widespread white matter degeneration preceding the onset of dementia. Alzheimer's & dementia: the journal of the Alzheimer's Association. 2015; 11:485–93 e2.
23. van Norden AG, de Laat KF, Gons RA, van Uden IW, van Dijk EJ, van Oudheusden LJ, et al. Causes and consequences of cerebral small vessel disease. The RUN DMC study: a prospective cohort study. Study rationale and protocol. BMC Neurol. 2011; 11:29. [PubMed: 21356112]

24. Tombaugh TN. Trail Making Test A and B: normative data stratified by age and education. Arch Clin Neuropsychol. 2004; 19:203–14. [PubMed: 15010086]
25. Van Der Elst W, Van Boxtel MP, Van Breukelen GJ, Jolles J. Assessment of information processing in working memory in applied settings: the paper and pencil memory scanning test. Psychol Med. 2007; 37:1335–44. [PubMed: 17376260]
26. Van der Elst W, Van Boxtel MP, Van Breukelen GJ, Jolles J. The Concept Shifting Test: adult normative data. Psychol Assess. 2006; 18:424–32. [PubMed: 17154763]
27. Duering M, Zieren N, Herve D, Jouvent E, Reyes S, Peters N, et al. Strategic role of frontal white matter tracts in vascular cognitive impairment: a voxel-based lesion-symptom mapping study in CADASIL. Brain. 2011; 134:2366–75. [PubMed: 21764819]
28. Zwiers MP. Patching cardiac and head motion artefacts in diffusion-weighted images. Neuroimage. 2010; 53:565–75. [PubMed: 20600997]
29. Smith SM, Jenkinson M, Woolrich MW, Beckmann CF, Behrens TE, Johansen-Berg H, et al. Advances in functional and structural MR image analysis and implementation as FSL. Neuroimage. 2004; 23(Suppl 1):S208–19. [PubMed: 15501092]
30. Smith SM, Jenkinson M, Johansen-Berg H, Rueckert D, Nichols TE, Mackay CE, et al. Tract-based spatial statistics: voxelwise analysis of multi-subject diffusion data. Neuroimage. 2006; 31:1487–505. [PubMed: 16624579]
31. Wollenweber FA, Baykara E, Zedde M, Gesierich B, Achmuller M, Jouvent E, et al. Cortical Superficial Siderosis in Different Types of Cerebral Small Vessel Disease. Stroke. 2017; 48:1404–7. [PubMed: 28364025]
32. Core Team, R. A language and environment for statistical computing. Vienna, Austria: R Foundation for Statistical Computing; 2016.
33. Sing T, Sander O, Beerenwinkel N, Lengauer T. ROCR: visualizing classifier performance in R. Bioinformatics. 2005; 21:3940–1. [PubMed: 16096348]
34. Fox, J., Weisberg, S. An R Companion to Applied Regression. 2nd. Thousand Oaks (CA): Sage; 2011.
35. Yoo W, Mayberry R, Bae S, Singh K, Peter He Q, Lillard JW Jr. A Study of Effects of MultiCollinearity in the Multivariable Analysis. Int J Appl Sci Technol. 2014; 4:9–19. [PubMed: 25664257]
36. Ranucci M, Castelvecchio S, Menicanti L, Frigiola A, Pelissero G. Accuracy, calibration and clinical performance of the EuroSCORE: can we reduce the number of variables? Eur J Cardiothorac Surg. 2010; 37:724–9. [PubMed: 19819158]
37. Strobl C, Malley J, Tutz G. An introduction to recursive partitioning: rationale, application, and characteristics of classification and regression trees, bagging, and random forests. Psychol Methods. 2009; 14:323–48. [PubMed: 19968396]
38. Strobl C, Boulesteix AL, Zeileis A, Hothorn T. Bias in random forest variable importance measures: illustrations, sources and a solution. BMC Bioinformatics. 2007; 8:25. [PubMed: 17254353]
39. Strobl C, Boulesteix AL, Kneib T, Augustin T, Zeileis A. Conditional variable importance for random forests. BMC Bioinformatics. 2008; 9:307. [PubMed: 18620558]
40. Prins ND, van Dijk EJ, den Heijer T, Vermeer SE, Jolles J, Koudstaal PJ, et al. Cerebral small-vessel disease and decline in information processing speed, executive function and memory. Brain. 2005; 128:2034–41. [PubMed: 15947059]
41. Zieren N, Duering M, Peters N, Reyes S, Jouvent E, Herve D, et al. Education modifies the relation of vascular pathology to cognitive function: cognitive reserve in cerebral autosomal dominant arteriopathy with subcortical infarcts and leukoencephalopathy. Neurobiol Aging. 2013; 34:400–7. [PubMed: 22626524]
42. Reyahi A, Nik AM, Ghiami M, Gritli-Linde A, Ponten F, Johansson BR, et al. Foxf2 Is Required for Brain Pericyte Differentiation and Development and Maintenance of the Blood-Brain Barrier. Dev Cell. 2015; 34:19–32. [PubMed: 26120030]
43. Tomimoto H, Akiguchi I, Suenaga T, Nishimura M, Wakita H, Nakamura S, et al. Alterations of the blood-brain barrier and glial cells in white-matter lesions in cerebrovascular and Alzheimer's disease patients. Stroke. 1996; 27:2069–74. [PubMed: 8898818]

44. Young VG, Halliday GM, Kril JJ. Neuropathologic correlates of white matter hyperintensities. Neurology. 2008; 71:804–11. [PubMed: 18685136]
45. Bridges LR, Andoh J, Lawrence AJ, Khoong CH, Poon WW, Esiri MM, et al. Blood-brain barrier dysfunction and cerebral small vessel disease (arteriolosclerosis) in brains of older people. J Neuropathol Exp Neurol. 2014; 73:1026–33. [PubMed: 25289893]
46. Wardlaw JM, Doubal F, Armitage P, Chappell F, Carpenter T, Munoz Maniega S, et al. Lacunar stroke is associated with diffuse blood-brain barrier dysfunction. Ann Neurol. 2009; 65:194–202. [PubMed: 19260033]
47. Topakian R, Barrick TR, Howe FA, Markus HS. Blood-brain barrier permeability is increased in normal-appearing white matter in patients with lacunar stroke and leucoaraiosis. Journal of neurology, neurosurgery, and psychiatry. 2010; 81:192–7.
48. Zhang CE, Wong SM, van de Haar HJ, Staals J, Jansen JF, Jeukens CR, et al. Blood-brain barrier leakage is more widespread in patients with cerebral small vessel disease. Neurology. 2016
49. Taheri S, Gasparovic C, Huisa BN, Adair JC, Edmonds E, Prestopnik J, et al. Blood-brain barrier permeability abnormalities in vascular cognitive impairment. Stroke. 2011; 42:2158–63. [PubMed: 21719768]
50. Highley JR, Gebril OH, Simpson JE, Wharton SB, Kirby J, Matthews F, et al. Axonal Preservation in Deep Subcortical White Matter Lesions in the Ageing Brain. Journal of Aging Science. 2014; 2:118.
51. Yates AJ, Thelmo W, Pappius HM. Postmorten changes in the chemistry and histology of normal and edematous brains. Am J Pathol. 1975; 79:555–64. [PubMed: 1137004]

Author Manuscript

Author Manuscript

Author Manuscript

Highlights

- Diffusion alterations in small vessel disease are mostly driven by free water
- White matter fiber organization seems relatively preserved
- Increased free water is strongly associated with clinical deficits
- Results were consistent across genetically defined SVD and sporadic SVD

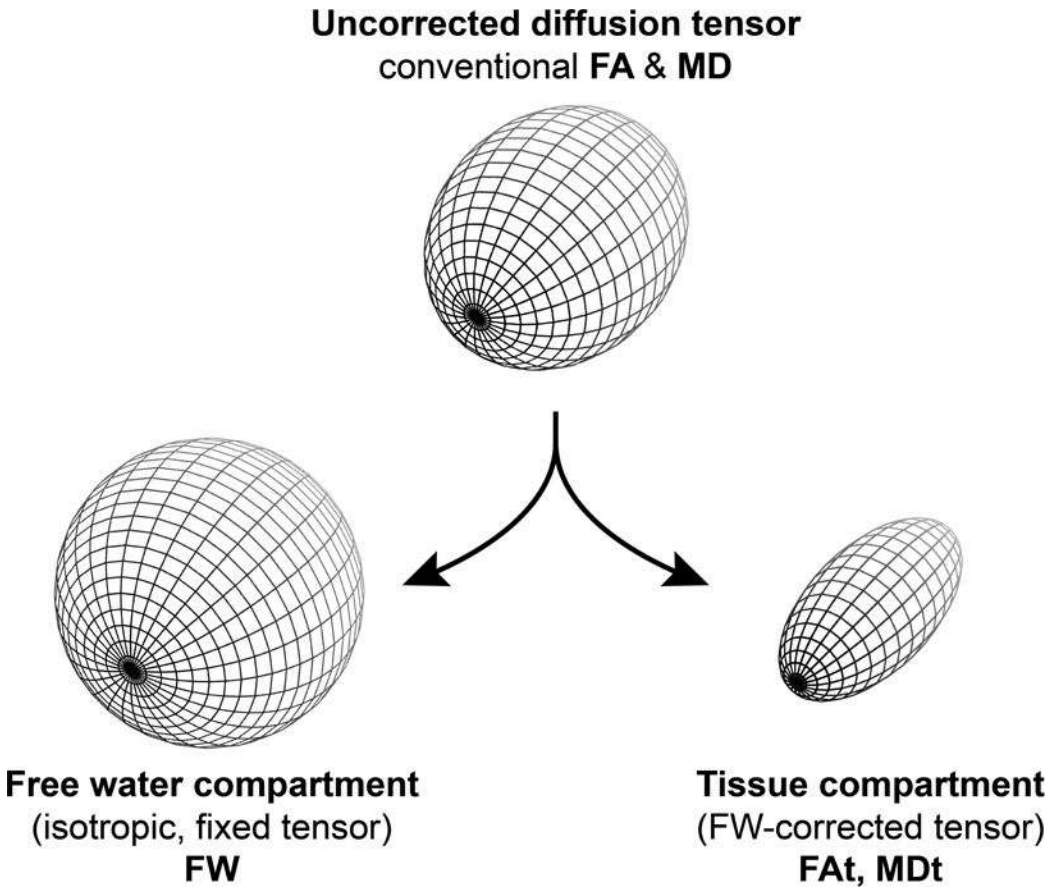

Figure 1. Free water imaging principle

Free water (FW) is modelled by an isotropic tensor with fixed diffusion coefficient of freely diffusing water at 37°C. The fractional volume of FW is used for quantification. After removal of the FW contribution, the tissue compartment is modeled on the remaining signal by a second tensor. The tissue compartment measures (FAt, MDt) are calculated from this second tensor.

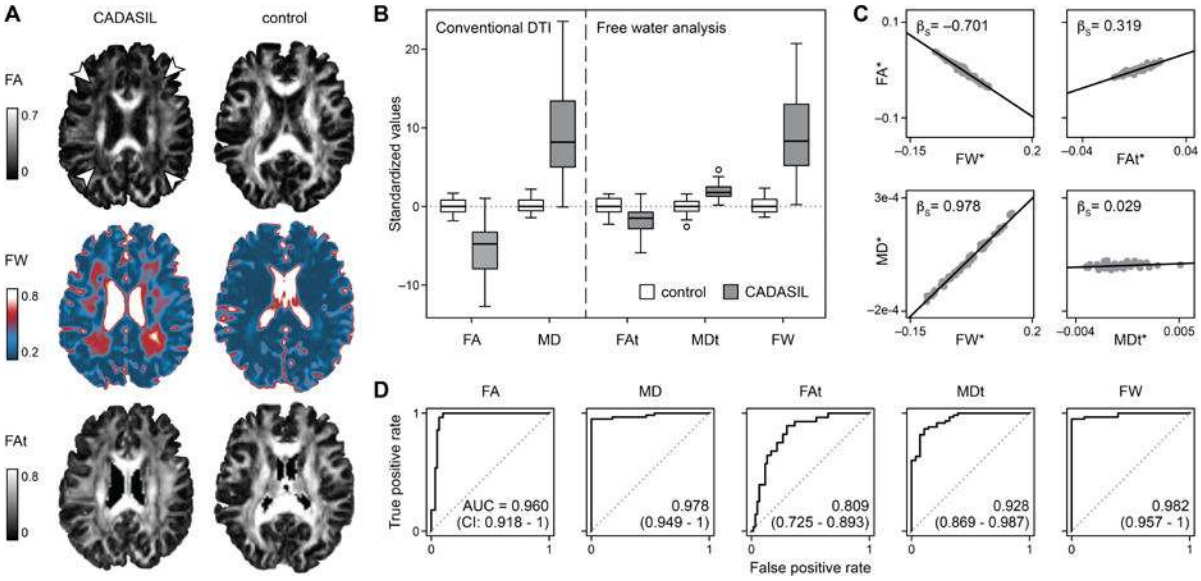

Figure 2. Free water imaging in CADASIL

A. Conventional FA, FW map and tissue compartment FAt for a representative CADASIL patient and control subject. **B**. Diffusion measures in control subjects and CADASIL patients within main fiber tracts. Standardized values (controls as reference) are presented as box plots. The decrease in FA and increase in MD is less pronounced after removing the FW contribution (tissue compartment FAt and MDt) while FW is prominently increased (group comparisons between CADASIL and controls all $P<1\times10^{-6}$, Wilcoxon rank sum tests). **C**. Partial regression analyses on both conventional FA and MD with FW and the respective tissue compartment measures (tissue compartment FAt and MDt) as independent variables. *variable corrected for all other variables (added variable plot). β_S, standardized beta from multiple linear regression. **D**. Receiver operator curves (ROC) illustrating the utility of DTI parameters as diagnostic biomarkers. Classification accuracy is quantified by the area under the curve (AUC) with 95% confidence interval (CI) after 5-fold cross validation.

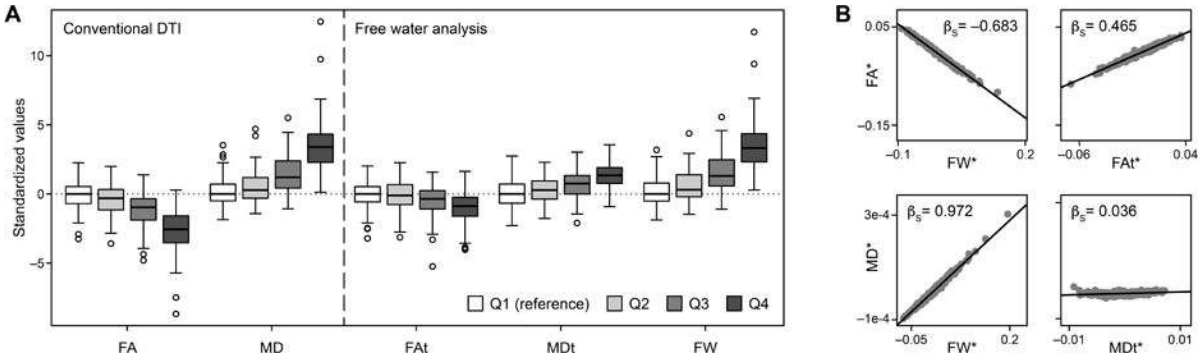

Figure 3. Free water imaging in sporadic small vessel disease

A. Box plots of standardized diffusion measures within main fiber tracts after stratifying the entire sample into quartiles (1st quartile Q1 to 4th quartile Q4) according to WMH burden. The decrease in FA and increase in MD from Q1 to Q4 is less pronounced after removing the FW contribution (tissue compartment FAt and MDt) while FW is prominently increased (group comparisons across quartiles all $P<1\times10^{-9}$, Kruskal-Wallis rank sum test) **B**. Partial regression analyses on both conventional FA and MD with FW and the respective tissue compartment measures (FAt and MDt) as independent variables. *variable corrected for all other variables (added variable plot). β_S, standardized beta from multiple linear regression.

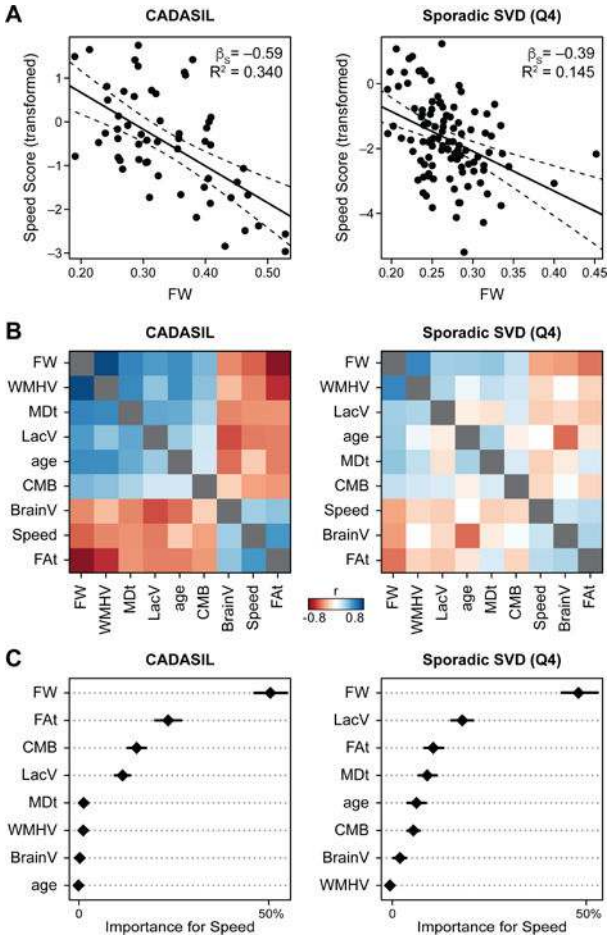

Figure 4. Associations between MRI markers and processing speed. A

Results from simple linear regression analyses between FW and processing speed scores for CADASIL patients (left) and sporadic SVD patients with high WMH burden (4th quartile Q4, right). The dashed line depicts the 95% confidence interval. β_S, standardized beta. **B**. Correlation matrix illustrating the high degree of intercorrelation between variables. **C**. Random forest regressions for estimating the importance of independent variables with regard to processing speed (dependent variable) while accounting for all other variables (conditional importance). Lines indicate the 95% confidence interval for the conditional variable importance measure calculated from 400 repetitions. Abbreviations: BrainV, normalized brain volume; CMB, cerebral microbleed count; FW, free water; FA, fractional anisotropy; FAt, tissue compartment FA; MD, mean diffusivity; MDt, tissue compartment MD; LacV, normalized lacune volume; WMHV, normalized white matter hyperintensity volume.

Table 1

Characteristics of the samples

	CADASIL (Munich)	Controls (Munich)	Sporadic SVD (RUN DMC)	*P**
n	57	28	444	–
Demographic characteristics				
Age, mean (SD) (min, max) [years]	53.4 (10.7) (29, 72)	70.5 (4.9) (60, 77)	65.3 (8.9) (49, 85)	< 0.001 a,c
Female, *n* (%)	38 (66.6)	18 (64.3)	201 (45.3)	0.002 c
Vascular risk factors, ***n (%)***				
Current smoker	11 (19.3)	3 (10.7)	69 (15.5)	0.388
Past smoker	24 (42.1)	14 (50.0)	239 (53.8)	0.243
Hypertension	13 (22.8)	12 (42.9)	320 (72.1)	< 0.001 c
Hypercholesterolemia	24 (42.1)	11 (39.3)	194 (43.7)	0.901
Diabetes	0 (0)	0 (0)	61 (13.7)	< 0.001 c
Processing speed z-scores, † ***median (IQR) (min, max)***				
TMT-A	−0.50 (1.61) (−13.2, 1.34)	0.39 (0.87) (−1.79, 1.79)	–	< 0.001
TMT-B	−0.48 (3.05) (−11.6, 1.72)	0.51 (1.56) (−2.11, 1.85)	–	< 0.001
1-letter P&P MST	–	–	−0.18 (1.44) (−8.08, 3.64)	–
LDST	–	–	−0.38 (2.17) (−3.74, 4.47)	–
Speed score‡	−0.56 (2.33) (−12.4, 1.16)	0.46 (0.77) (−1.16, 1.69)	−0.31 (1.59) (−5.26, 4.06)	< 0.001 a,b
Conventional SVD imaging markers, ***median (IQR) (min, max)***				
WMH volume [%]§	7.38 (7.53) (0.09, 22.8)	0.13 (0.14) (0, 1.48)	0.59 (1.23) (0.05, 14.0)	< 0.001 a,b,c
Lacune volume [%]§	0.02 (0.06) (0, 0.25)	0 (0) (0, 0)	0 (0) (0, 0.10)	< 0.001 a,c
Brain volume [%]§	78.4 (6.86) (70.0, 87.2)	73.2 (5.99) (66.4, 79.1)	65.4 (7.76) (49.9, 80.9)	< 0.001 b,c
Cerebral microbleeds	0 (3) (0, 118)	0 (0) (0, 0)	0 (0) (0, 36)	< 0.001 a,c

* post-hoc tests with $P < 0.01$ after correction for multiple comparisons are indicated with letters, a: CADASIL vs. Controls, b: Sporadic SVD vs. Controls, c: CADASIL vs. Sporadic SVD.

† age and education adjusted z-scores;

‡ compound z-score;

§ normalized by the intracranial volume; Abbreviations: IQ, interquartile range; LDST, letter digit substitution test; P&P MST, paper pencil memory scanning test; SD, tandard deviation; TMT, trail making test; WMH, white matter hyperintensity

Table 2

Simple linear regression with processing speed

Regressor	β_S*	*P*	R^2[%]
CADASIL			
Free water (FW)	−0.594	1.14×10^{-6}	34.0
Tissue compartment FAt	0.584	1.83×10^{-6}	32.9
Lacune volume†	−0.514	4.31×10^{-5}	25.1
WMH volume†	−0.481	1.52×10^{-4}	21.7
Tissue compartment MDt	−0.457	3.51×10^{-4}	19.5
Cerebral microbleeds	−0.407	.00166	15.1
Brain volume†	0.349	.00776	10.6
age	−0.398	.056	4.8
Sporadic SVD, whole sample			
Free water (FW)	−0.272	7.12×10^{-9}	7.4
Tissue compartment FAt	0.235	6.24×10^{-7}	5.5
WMH volume†	−0.192	5.20×10^{-5}	3.7
Brain volume†	0.172	2.95×10^{-4}	3.0
Lacune volume†	−0.165	5.23×10^{-4}	2.7
Tissue compartment MDt	−0.150	.00167	2.2
Cerebral microbleeds	−0.150	.00169	2.2
age	−0.117	.0145	1.4
Sporadic SVD, WMH volume 4th quartile (Q4)			
Free water (FW)	−0.392	3.03×10^{-5}	14.5
Tissue compartment FAt	0.266	.00569	6.2
Lacune volume†	−0.247	.0104	5.2
Tissue compartment MDt	−0.234	.0152	4.6
Brain volume†	0.214	.0272	3.7
WMH volume†	−0.202	.0371	3.2
Cerebral microbleeds	−0.201	.0377	3.1
age	0.008	.938	0.0

*standardized beta;

†normalized by the intracranial volume; Abbreviations: FA, fractional anisotropy; MD, mean diffusivity; WMH, white matter hyperintensity